

Analytical Methods

Accepted Manuscript

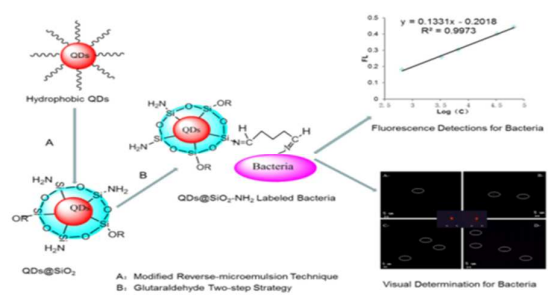


This is an *Accepted Manuscript*, which has been through the Royal Society of Chemistry peer review process and has been accepted for publication.

Accepted Manuscripts are published online shortly after acceptance, before technical editing, formatting and proof reading. Using this free service, authors can make their results available to the community, in citable form, before we publish the edited article. We will replace this *Accepted Manuscript* with the edited and formatted *Advance Article* as soon as it is available.

You can find more information about *Accepted Manuscripts* in the [Information for Authors](#).

Please note that technical editing may introduce minor changes to the text and/or graphics, which may alter content. The journal's standard [Terms & Conditions](#) and the [Ethical guidelines](#) still apply. In no event shall the Royal Society of Chemistry be held responsible for any errors or omissions in this *Accepted Manuscript* or any consequences arising from the use of any information it contains.



Hydrophobic CdSe/ZnS were incorporated into SiO₂ spheres, and amine-modified CdSe/ZnS@SiO₂ nanoparticles were used for quantitative and visual determination of bacteria.

ARTICLE

Sensitive Quantification and Visual Detection of Bacteria Using CdSe/ZnS@SiO₂ Nanoparticles as Fluorescence Probe

Cite this: DOI: 10.1039/x0xx00000x

Renjie Wang,^a Yi Xu,^{*a b c} Yan Jiang,^a Na Chuan,^a Xi Su,^a Jingou Ji^a

Received 00th January 2012,

Accepted 00th January 2012

DOI: 10.1039/x0xx00000x

www.rsc.org/

CdSe/ZnS@SiO₂-NH₂ composite nanoparticles (FNPs) were proposed and used as fluorescent markers for bacteria detection, *Salmonella typhimurium* acted as representative sample in this paper. It was shown that the hydrophobic CdSe/ZnS quantum dots (QDs) were incorporated into SiO₂ spheres by using self-modified reverse-microemulsion technique. The FNPs could be covalently conjugated with the bacteria by glutaraldehyde two-step strategy successfully. A good linear relationship between the concentration of *Salmonella typhimurium* and fluorescence intensity was obtained in the range of $6.6 \times 10^2 \sim 6.6 \times 10^4$ cfu mL⁻¹, and the equation was just as $I = 0.1331 \log C - 0.2017$ with $R^2 = 0.9974$. The detection limit was 3.3×10^2 cfu mL⁻¹, and this method could be applied to other bacteria detection as well. In order to further reduce the detection limit and achieve better visual determination performance, an integrated dielectrophoresis (DEP) microfluidic chip and relative microsystem was established. The FNPs-labeled bacteria could be enriched along the edges of the interdigitated microelectrodes in the micro-channel by positive DEP and could be counted under the fluorescence microscope.

Introduction

Food-borne pathogens are widely distributed and directly influence the health of mankind.¹ The situation in developing countries is even more serious, for instance, the mortality rate of *Salmonella* infection in developing countries is 24% higher than that in developed countries.² Bacteria detection is one of the most important criteria in the fields of food safety, environmental monitoring, clinical diagnosis, etc. However, there are some shortcomings for the conventional methods. For example, plate count method is time-consuming, labor intensive, and lack of sensitivity. Although enzyme-linked immunosorbent assays (ELISA)³⁻⁴ and polymerase chain reaction (PCR)⁵⁻⁶ are of characters such as higher sensitivity and selectivity, they are still limited by complex sample pretreating and result instability. Therefore, fluorimetry with its own higher accuracy and reliability has been widely applied for bacteria detection.⁷⁻¹⁰

Hydrophobic quantum dots (QDs) have become the preferred sensitive fluorescent reagent for their benefits of perfect crystal and bright fluorescence in the fluorescence detection.¹¹ In practical application, much more attention has been paid to ensure the efficiency of fluorescent as well as to improve their biocompatibility and stability.

Bardelang et al. proposed to immobilize dipeptide on the surface of core/shell CdSe/ZnS QDs which could provide better biocompatibility.¹² Because dipeptide tended to decrease the size of QDs, and made fluorescence peak blue-shift, so the performance of QDs was influenced inevitably. Surface ligand-exchange¹³ or incorporating QDs into macromolecular material¹⁴ were often used to enhance the biocompatibility of hydrophobic QDs. Unfortunately, those methods also led to a huge loss in fluorescence due to the change of QDs surface-properties. Further research indicated that SiO₂ could be used to wrap the QDs and other fluorescent reagents with the features of high stability and transparency, and it also shows superior performance and promising applications.¹⁵

Reverse microemulsion method has been developed to incorporate hydrophilic QDs and fluorescent reagent into SiO₂ beads.¹⁶⁻¹⁷ For example, He¹⁸ and Zhao¹⁹ used the RuBpy-doped silica nanoparticles as fluorescence probe to test the levels of *Salmonella typhimurium* and *Escherichia coli*. Using reverse microemulsion method to incorporate hydrophobic QDs into silica spheres has aroused researchers' great interest. Koole²⁰ and Zhelev²¹ showed strong experimental evidence in favor of the feasibility of hydrophobic QDs into monodisperse silica spheres by this way. The silica surface could not only prevent oxygen penetration and reduce the toxicity of QDs, but also be

easily modified with different functional groups such as amines, thiols, carboxys, etc. Fluorescent nanoparticles prepared by this method were of tunable size and preferable optical property, and facilitated to the biomedical applications, such as live-cell imaging²², fingerprint detection²³, molecule tracing²⁴.

Until now, there are few researches about QDs@SiO₂ nanoparticles used as fluorescent probe for bacterium detection and visual observation. It is difficult to directly and effectually observe the bacteria by the microscope since the bacteria were incredibly small. In order to achieve better visualization and detection of the bacteria, the integrated DEP microfluidic chip was proposed to capture and enrich the target bacteria.²⁵⁻²⁸ Yang et al. demonstrated that positive DEP could concentrate *Listeria* efficiently at the edges of the interdigitated micro-electrodes from the flow in microfluidic channels.²⁹ So, bacteria visualizations were worth further study by using high efficient fluorescent markers and integrated dielectrophoresis microfluidic chip.

A high sensitive method for bacterium determination was developed in this paper. CdSe/ZnS@SiO₂-NH₂ composite nanoparticles (FNPs) prepared by self-modified reverse-microemulsion technique were used as highly efficient fluorescent markers and glutaraldehyde was used as crosslinker. FNPs could successfully be covalently conjugated with the bacteria by two-step crosslinking strategy. In order to further improve the detection sensitivity and achieve visual determination, positive DEP was proposed to capture small amounts of FNPs-labeled bacteria efficiently to edges of interdigitated micro-electrodes. With the signal amplification of FNPs, bacteria could be visualized and counted under a fluorescence microscope.

Experimental

Instruments and Reagents

Fluorescence spectrometer (RF-5301, SHIMADZU), Fourier transform infrared spectrometer (IRprestige-21, SHIMADZU), Laser Particle Size Analyzers (Zetasizer Nano ZS90, Malvern), Thermo fluoroskan ascent FL (Thermo Scientific), Syringe pump (55226, HARVARD Apparatus), Inverted fluorescence Microscope (IX71, OLYMPUS), Arbitrary waveform generator (33220A, Agilent). Tetraethoxysilane (TEOS), TritonX-10, (3-aminopropyl)triethoxysilane (APTES), 3-(Trihydroxysilyl)propylmethylphosphonate (THPMP) were purchased from J&K Chemical Ltd. CdSe/ZnS quantum dots powder was purchased from Ocean NanoTech.

Salmonella typhimurium, *Escherichia coli* and *Staphylococcus aureus* used in the experiment were provided by College of laboratory medicine, Chongqing Medical University. Strains were transferred into Luria Bertani broth and incubated at 37 °C for 12 h prior to use. The initial concentration of each bacteria was obtained using plate count method respectively. The mixed bacteria was composed of a certain amount of the three kinds of bacteria.

Synthesis of CdSe/ZnS@SiO₂-NH₂ nanoparticles

TritonX-100 (1.77 mL), 1-Hexyl alcohol (1.80 mL), cyclohexane (7.50 mL) and hydrophobic CdSe/ZnS quantum dots (0.75 mg) were added in a flask, ultrasonic dispersion uniformity, then TEOS (100 µL) was added into the flask under vigorous stirring. Thirty minutes after the microemulsion system was formed, ammonia solution (60 µL, 25 wt%) was introduced to initiate and catalyze the polymerization process. The silica growth was completed after 24 hours stirring at room temperature. Chemically activated CdSe/ZnS@SiO₂ were prepared by adding APTES (20 µL) and THPMP (40 µL) for the introduction of amino groups after another 24 hours of polymerization. The resulting CdSe/ZnS@SiO₂-NH₂ nanoparticles were isolated from the microemulsion using acetone and centrifuged, and the resultant precipitates of particles were washed by centrifuging with 4500 rpm for 5 min, washed for two times by ethanol and once by pure water to remove any surfactant and unreacted molecules, and placed under the conditions of protection from light vacuum drying in low temperature for further application.

Characterization of CdSe/ZnS@SiO₂-NH₂ nanoparticles

Fluorescence spectra of CdSe/ZnS and CdSe/ZnS@SiO₂-NH₂ were recorded on RF-5301 Fluorescence spectrometer. The structure, size, and morphology of the resulting nanoparticles were determined by transmission electron microscopy (JEM-100CXII, Japan). Infrared measurements were performed on an IRprestige-21 spectrometer at room temperature. A small amount (1~5 mg) of each sample was triturated with KBr in order to prepare the pellet for IR measurements. The Zeta potential of nanoparticles was measured by the Laser Particle Size Analyzers.

Covalent immobilization of CdSe/ZnS@SiO₂-NH₂ nanoparticles onto bacteria surfaces and fluorescence detection

Two-step strategy operation: FNPs (5 mg) were dispersed into the PBS (400 µL, 0.01 M), and then glutaraldehyde (400 µL, 1.25%) was added. After 2 hours at RT, the nanoparticles were washed by centrifugation to remove excess glutaraldehyde. After the nanoparticles were redispersed in PBS, they were further incubated with bacteria (400 µL) for 4 hours at room temperature with gentle shaking. Finally, the mixtures were purified by using ultrafiltration membrane (0.22 µm) to wash away the excess FNPs, until no fluorescence signal was found in the last filtrate.

One-step strategy operation: FNPs (5 mg) were dispersed into the PBS (400 µL, 0.01 M) buffer, and then glutaraldehyde (400 µL, 1.25%) and bacteria were added at the same time, the mixture was incubated at RT for 4 h with gentle shaking. The purification process remains the same.

Serial dilutions of *Salmonella typhimurium* labeled with FNPs (300 µL) prepared by the above two approaches suspended in DI water with concentration of 3.3×10^2 cfu mL⁻¹, $6.6 \times 10^2 \sim 6.6 \times 10^4$ cfu mL⁻¹ were respectively introduced into 96-well plates (N = 6) for quantitative analysis by Thermo fluoroskan ascent FL.

Visual detection of CdSe/ZnS@SiO₂-NH₂ labeled bacteria with dielectrophoretic enrichment in the micro-fluidic chip

The FNPs-labeled bacteria samples were diluted in a series with concentration of 200, 400, 800, 1600 cfu mL⁻¹, so there were separately about 5, 10, 20, 40 cells per 25 μ L sample measured by micro-syringe. At the beginning of dielectrophoretic enrichment, a modest amount of deionized water was injected into the DEP channels by using a syringe pump at a flow rate of 0.3 μ L min⁻¹ to completely discharged bubbles, then the 25 μ L of bacteria samples with different concentration were injected into the DEP channel at the same rate when a 6 Vpp was applied to the interdigitated electrodes at a frequency of 100 KHz by an arbitrary waveform generator. After enrichment, the visualization of bacteria counting could be attained using the CCD microscope imaging detection system.

Results and discussion

Preparation and characterization of CdSe/ZnS@SiO₂-NH₂ nanoparticles

The hydrophobic QDs in silica spheres prepared by reverse microemulsion synthesis could be explained with two hypothetical mechanisms.¹⁶ (1) The hydrophobic QDs could be wrapped by the surfactant and transferred into aqueous phase of the microemulsion, after the ammonia catalyst was added; the TEOS was able to hydrolyze on the particle surfaces only in aqueous phase and incorporate QDs into SiO₂ shell. (2) When TEOS solution was added into organic solution, they had an affinity for the QDs surface; the hydrophobic groups of the QDs were exchanged with TEOS to obtain silanized QDs. After the hydrophilic surface was formed, silanized QDs transferred to hydrophilic phase of the microemulsion, and generated SiO₂ layers by using hydrolysis of TEOS on the silanized QDs in the present of ammonia catalyst. Furthermore, SiO₂ layer could grow in situ by adsorbing subsequently hydrolyzed TEOS³⁰⁻³³. Considering the mechanisms of incorporate hydrophobic or hydrophilic QDs coating with SiO₂ shells by the reverse microemulsion, the key difference between them was the adding order of ammonia catalyst. Firstly, it was sure that the hydrophobic QDs were fully dispersed in the solution composed of surfactant and oil phase. TEOS was added under vigorous stirring to ensure that it could contact with QDs fully, and then ammonia solution was introduced into the reaction system. It could not only provide the site of the hydrolysis reaction, but also initiate and catalyze the polymerization process (Fig. 1A).

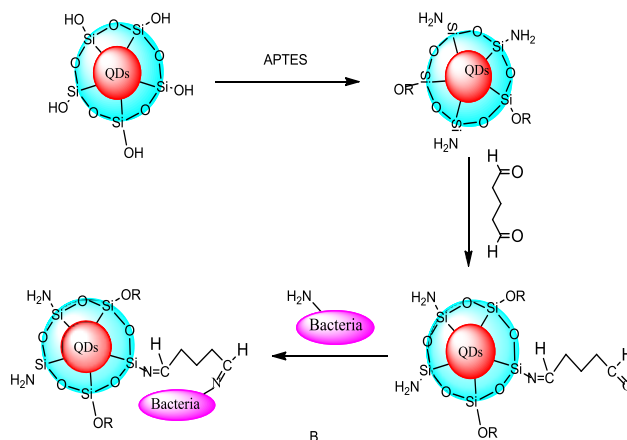
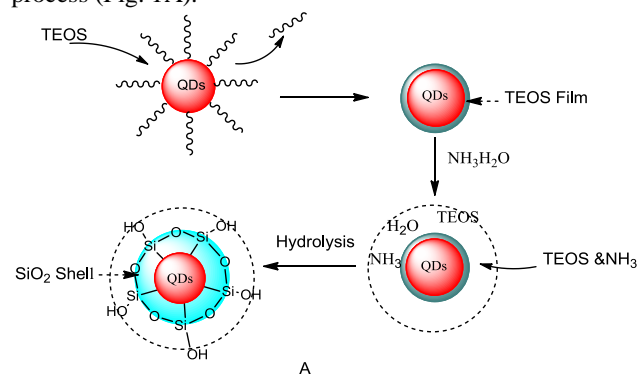


Fig. 1. (A) Synthetical process of CdSe/ZnS@SiO₂ composite nanoparticles. (B) Conjugation process between CdSe/ZnS@SiO₂-NH₂ and target bacteria

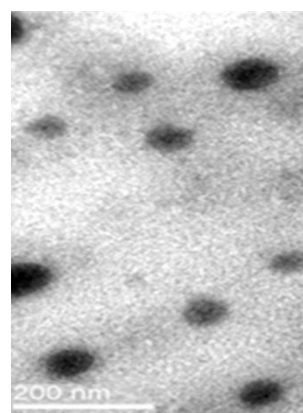


Fig. 2. TEM image of the silica-coated CdSe/ZnS nanoparticles

The silica shell could be modified with a variety of functional groups for the existence of -OR groups. To facilitate the bacterial detection, APTES was proposed as amination reagent and some -OH groups on the surface of SiO₂ could be replaced by -NH₂ groups in the reaction and amine-modified nanoparticles were obtained. In order to prevent the agglomeration of nanoparticles and keep them in better dispersal state, methylphosphonate was introduced onto the surface of composite nanoparticles as inert stabilizing groups which could effectively decrease the aggregation of the nanoparticles³⁴ by electrostatically interacting with the majority of amino groups. Since a lot of amine groups on the surface of bacteria were free, multiple amine-modified nanoparticles could be bound to one bacterium by glutaraldehyde, (Fig. 1 B)

The TEM image of FNPs was shown in Fig. 2. It demonstrated that the silica-shelled QDs nanoparticles were monodisperse and quite uniform in size with diameter 70 nm. The FTIR spectras of FNPs and CdSe/ZnS nanoparticles were shown in Fig. 3. The IR absorption peaks at 1065.99 cm⁻¹ and 910.40 cm⁻¹ were stretching vibrational absorption of Si-O-Si and Si-OH, and the peak near 790 cm⁻¹ was attributed to the bending stretching of Si-O-Si. Those indicated that SiO₂ shell was formed and the characteristic bands at 3540-3125 cm⁻¹ showed the amine groups were introduced successfully. Furthermore, the zeta potential of FNPs turned positive to -2.56 mV from -31.9 mV after amine was introduced (Table S1,

Supplementary Information), which showed that the structure of FNP s conformed to our designed requirements.

The fluorescence spectras of CdSe/ZnS QDs and FNP s were shown in Fig. 4. It was illustrated that the peak shape was symmetrical and position of the emission peak hardly changed, and the half width of the peak only increased 6 nm. The fluorescence emission intensity has declined slightly, which might be explained by the block of SiO₂ shell and the changes of luminescence property of the QDs. As known, silica layer was usually porous, and the free group (RO-) produced in the hydrolyzation process could dissolve in the aqueous medium and slowly penetrate the silica shell, which led to the quantum yield loss of the encapsulated QDs.³² Therefore, it is very important to optimize the SiO₂ coating process to reduce the fluorescence loss.

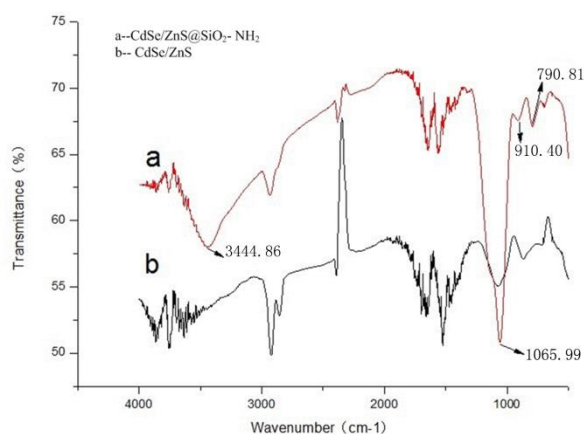


Fig. 3. FTIR spectra of CdSe/ZnS@SiO₂-NH₂ nanoparticles (a) and CdSe/ZnS QDs (b)

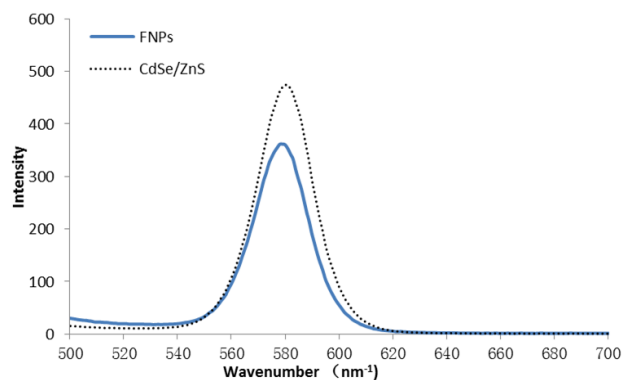


Fig. 4. Fluorescence spectra of CdSe/ZnS and FNP s

Coupling process of CdSe/ZnS@SiO₂-NH₂ nanoparticles with *Salmonella typhimurium* and its detection

It's known that the crosslink process with glutaraldehyde (GA) as cross linking agent included one-step strategy and two-step strategy.³⁵⁻³⁶ In the one-step process, GA simultaneously reacted with the amine groups of nanoparticles and *Salmonella typhimurium*. In the two-step strategy, GA reacted with nanoparticles and subsequently connected to the *Salmonella*

typhimurium (Fig. 1 B). FNP s were taken as fluorescent marker, and shown stronger fluorescent signals which made it possible to detect bacteria quantitatively.

The results of both labeling strategies were shown in Fig. 5. The fluorescence signals of serial dilutions of *Salmonella typhimurium* labeled with FNP s were obtained and compared. It indicated that stronger signals and better linear relationship ($R^2 = 0.9974$) were obtained in two-step strategy. This was because every reaction in the process of two-step crosslinking could be carried out adequately. Firstly, the reaction between high concentrations of glutaraldehyde and amine groups on the nanoparticles was completely finished. Then, excess glutaraldehyde could be removed by centrifugation, and a number of aldehyde groups on the surface of nanoparticles were free, which could further react with the *Salmonella typhimurium* and nanoparticles were connected to *Salmonella typhimurium* by five carbon bridge eventually. While in one-step strategy, nanoparticles and *Salmonella typhimurium* were added into glutaraldehyde solution simultaneously, the amine groups on *Salmonella typhimurium* would react with glutaraldehyde beside the reaction between FNP s and glutaraldehyde. Under same conditions the chances of linking nanoparticles with *Salmonella typhimurium* would undoubtedly be reduced. So glutaraldehyde two-step strategy gained an advantage over one-step strategy in bacteria crosslink process, and in order to get better fluorescent signals, the two-step strategy should be adopted.

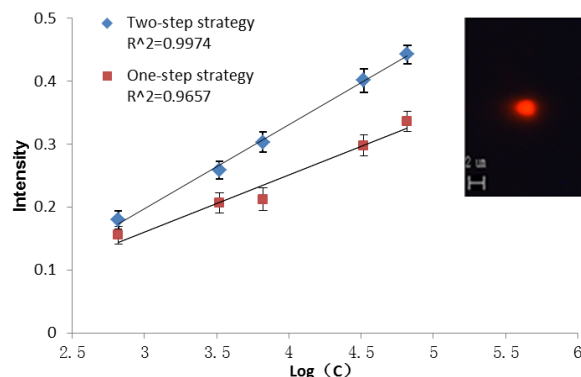


Fig. 5. Linear relationship of the fluorescence intensity vs the concentration of *Salmonella typhimurium* with the process of one-step strategy and the two-step strategy. The inset shown fluorescence image of *Salmonella typhimurium* after incubated with FNP s. The error bars represent standard deviations for N=6.

Fig. 5 showed that the linear range of FNP s-labeled *Salmonella typhimurium* with two-step strategy was from 6.6×10^2 to 6.6×10^4 cfu mL⁻¹, and the equation was $I = 0.1331 \log C - 0.2017$ with $R^2 = 0.99744$. The limit of detection was 3.3×10^2 cfu mL⁻¹, which was an order of magnitude lower than previous methods.

The repeatability and universality of the proposed method was evaluated. The results were shown in Table 1. It could be seen that the number of *Salmonella typhimurium*, *Escherichia coli* and *Staphylococcus aureus* measured by this method using the standard curve presented in fig. 5 was consistent with the conventional plate count method respectively, and the standard deviation (N=6) were satisfactory. This was taken as proof that this method could be used to detect different bacteria even mixed bacteria.

Table 1 Detection results of different stains

Samples	Plate count method (cfu mL ⁻¹)	Proposed method (cfu mL ⁻¹)
<i>Salmonella typhimurium</i>	4.3×10^4	$(4.0 \pm 0.2) \times 10^4$
<i>Escherichia coli</i>	8.6×10^3	$(8.4 \pm 0.4) \times 10^3$
<i>Staphylococcus aureus</i>	2.6×10^4	$(2.3 \pm 0.2) \times 10^4$
Mixed sample	3.7×10^3	$(3.7 \pm 0.5) \times 10^3$

Visual detection in the microfluidic chip

Based on outstanding fluorescent property of FNPs, FNPs-labeled *Salmonella typhimurium* was of superior recognition. With the help of pDEP, small amounts of FNPs-labeled *Salmonella typhimurium* could be collected to edges of interdigitated micro-electrodes and visualized under a fluorescence microscope. *Escherichia coli* and *Staphylococcus aureus* were detected in the experiment, the results of which were identical with those of *Salmonella typhimurium*, *Salmonella typhimurium* was just used as representative sample in here.

In order to assure enough contact area between bacteria-FNPs suspension and microelectrodes, the interdigitated microelectrodes (IME) were adopted in the DEP microchip (Fig. 6). The DEP microchip was assembled by two parts: an array of gold interdigitated microelectrode on a glass substrate and a cover with a channel formed by poly dimethylsiloxane (PDMS). The IME contained 25 pairs of opposing gold finger electrodes, and each electrode was 30 μm wide with a spacing of 20 μm . The PDMS layer was made by mixing the elastomer monomer and the curing agent at the ratio of 10:1 (w/w). By pouring the mixture evenly on the mold and curing at 90 $^{\circ}\text{C}$ 50 min, PDMS layer with the channel of 30 μm in width and 20 μm in depth was removed from the mold.

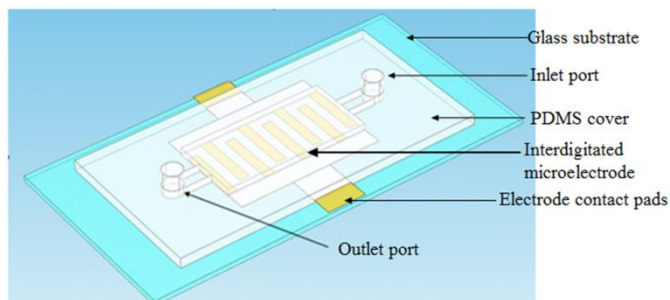


Fig. 6. Schematic of the micro-fluidic biochip used in this study

Bacteria labeled with FNPs still were of dielectric property, when its suspension were injected into the microchannel at the flow rate of 0.3 $\mu\text{L min}^{-1}$ on the DEP microchip, FNPs-labeled bacteria experienced positive DEP forces and were collected along the edges of interdigitated microelectrodes (IME), as was shown in Fig 7, under the conditions of 6 V excitation potential and 100 KHz induced frequency.

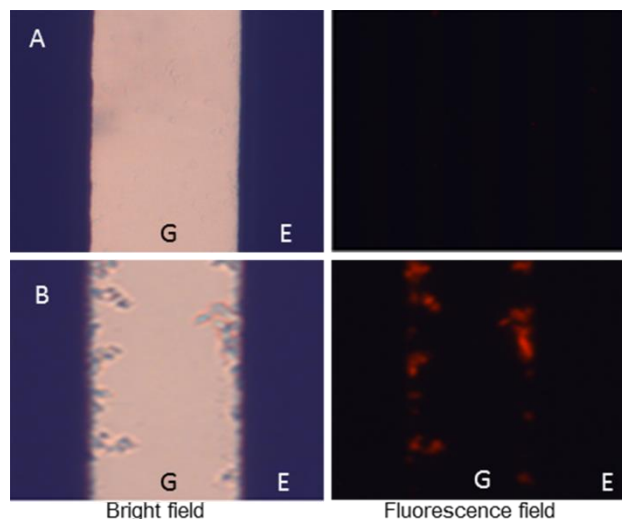


Fig. 7. (A) Image of *Salmonella typhimurium* labeled with FNPs without DEP. (B) 25 μL *Salmonella typhimurium*-FNPs sample with concentration of 10^4 cfu mL⁻¹, flow rate was 0.3 $\mu\text{L min}^{-1}$, DEP: 6 Vpp, 100 KHz. G refers to electrode gap, E refers to electrode.

The mixture of *Salmonella typhimurium* and FNPs without glutaraldehyde was injected into microchannel in the DEP chip under the same conditions. After DEP treatment, *Salmonella typhimurium* could be collected along the microelectrodes. However, the fluorescence signal was very weak (Fig. 8), it meant the fluorescence nanoparticles were not of dielectric property and unable to be captured by DEP in the experiment.

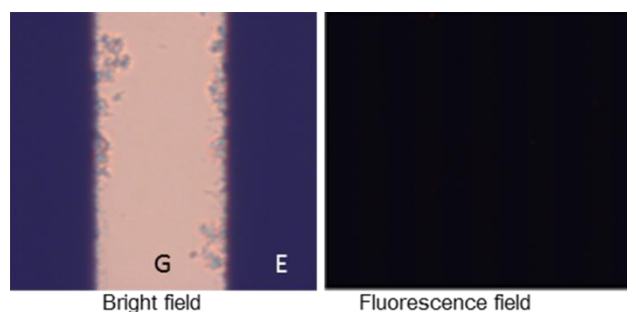


Fig. 8. Image of *Salmonella typhimurium* mixed with FNPs (5mg), Flow rate was 0.3 $\mu\text{L min}^{-1}$, DEP: 6 Vpp, 100 KHz.

The sample concentrations used for fluorescence visualization detection were 5 cells, 10 cells, 20 cells, 40 cells in volume of 25 μL , respectively. When sinusoidal voltage (6 Vpp with 100 KHz) was applied to the interdigitated electrodes, the FNPs-labeled *Salmonella typhimurium* could be captured on the electrode edges from the continuous flow by pDEP, and retained in the detection area. The detecting results were shown in Fig. 9 (only one picture of each concentration was displayed as representative). Single FNPs-labeled bacteria in fluorescence field could be observed with a limit of ca. 5 cells per 25 μL .

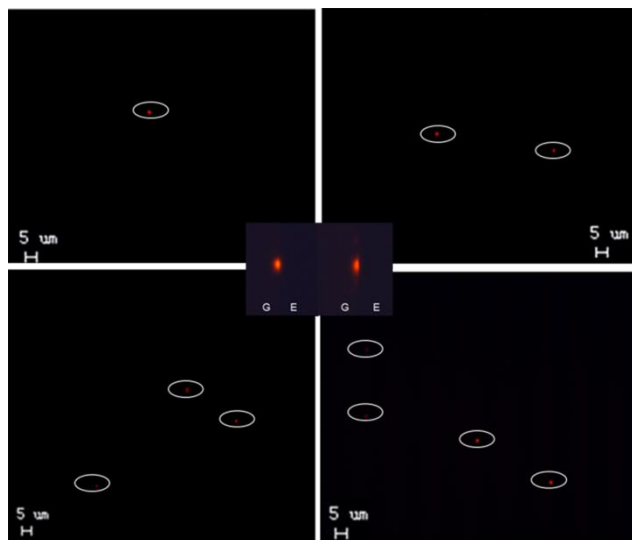


Fig.9. Fluorescence microscopic images of *Salmonella typhimurium* cells captured in the micro-channel by pDEP (Bacteria concentrations of the samples corresponding to panels A–D were 5, 10, 20, 40 cells per 25 μL).

Conclusions

Hydrophobic CdSe/ZnS QDs were incorporated into SiO_2 spheres by modified reverse microemulsion method, and the CdSe/ZnS@ SiO_2 nanoparticles were luminous, uniform and monodispersed. Amine-modified silica nanoparticles could be connected to bacteria by glutaraldehyde two-step strategy. A good linear relationship between the concentration of bacteria and fluorescence intensity was obtained in the range of $6.6 \times 10^2 \sim 6.6 \times 10^4 \text{ cfu mL}^{-1}$, the equation just as $I = 0.1331 \log C - 0.2017$ with $R^2 = 0.99744$, and the limit of detection was $3.3 \times 10^2 \text{ cfu mL}^{-1}$. The *Salmonella typhimurium* labeled by CdSe/ZnS@ $\text{SiO}_2\text{-NH}_2$ still kept dielectric property, and the FNP-labeled bacteria could be captured along the electrode edges from the continuous flow by pDEP. Hence, with the help of bright fluorescence of FNPs, the visualization of bacteria counting was attained under a fluorescence microscope.

Acknowledgements

This work was supported by the National Natural Science Foundation of China (No. 21375156), the Foundation for the Author of National Excellent Doctoral (FSNEDD-200941), and the Research Project of New Detection Technology for Toxic Substances and Illegal Additive in Food and Drug [CSTC, 2012ggB1001].

Notes and references

^a College of Chemistry and Chemical Engineering, Chongqing University, No. 174, St. Shazhengjie, Shapingba District, Chongqing, China.

Fax: (+86) 23 65111022; E-mail: xuyibbd@sina.com

^b National Center for International Research of Micro/Nano-System and New Material Technology, No. 174, St. Shazhengjie, Shapingba District Chongqing, China. Fax: (+86) 23 65111022; E-mail: xuyibbd@sina.com

^c Key Laboratory of Fundamental Science of Micro/Nano-Device and System Technology for National Defense, Chongqing, China. Fax: (+86) 23 65111022; E-mail: xuyibbd@sina.com

1 E. Scallan, R. M. Hoekstra, F. J. Angulo, R. V. Tauxe, M. A. Widdowson, S. L. Roy, J. L. Jones, P. M. Griffin, *Emerg Infect. Dis.*, 2011, 17, 7–15.

2 Y. Chimalizeni, K. Kawaza, E. Molyneux, A. Finn, N. Curtis, A. J. Pollard. 2010, The epidemiology and management of non typhoidal *Salmonella* typhimurium infections. In A. Finn, N. Curtis, & A. J. Pollard (Eds.), *Advances in experimental medicine and biology (hot topics in infection and immunity in children VI)* (pp. 33–46). New York: Springer

3 S. Jain, S. Chattopadhyay, R. Jackeray, C. K. V. Zainul Abid, G. S. Kohli, H. Singh, *Biosens and Bioelectron.*, 2012, 31, 37–43.

4 H. Hoon Cho, J. Irudayaraj, *Int. J. Food Microbiol.*, 2013, 164, 70–75.

5 N. J. Opet, R. E. Levin, *J. Microbiol Meth.*, 2013, 94, 69–72.

6 C. C. Liu, C. Y. Yeung, P. H. Chen, M. K. Yeh, S. Y. Hou, *Food Chem.*, 2013, 141, 2526–2532.

7 C. Y. Wen, J. Hu, Z. L. Zhang, Z. Q. Tian, G. P. Ou, Y. L. Liao, Y. Li, M. Xie, Z. Y. Sun, D. W. Pang, *Anal. Chem.*, 2013, 85, 1223–1230.

8 X. Fu, K. L. Huang, S. Q. Liu, *Anal Bioanal Chem.*, 2010, 396, 1397–1404.

9 X. J. Zhao, L. R. Hilliard, S. J. Mechery, Y. P. Wang, R. P. Bagwe, S. G. Jin, W. H. Tan, *PNAS.*, 2004, 101, 15027–15032.

10 C. C. Carrión, B. M. Simonet, M. Valcárcel, *Biosens and Bioelectron.*, 2011, 26, 4368–4374.

11 D. Bardelang, M. B. Zaman, I. L. Moudrakovski, S. Pawsey, *Adv. Mater.*, 2008, 20, 4517–4520.

12 Y. Zhu, Z. Li, M. Chen, H. M. Cooper, Z. P. Xu, *J. Mater. Chem. B.*, 2013, 1, 2315–2323.

13 P. D. Wadhavane, R. E. Galian, M. A. Izquierdo, J. A. Sigalat, *J. Am. Chem. Soc.*, 2012, 134, 20554–20563.

14 P. Mulvaney, L. M. Liz-Marzan, M. Giersig, T. Ung, *J. Mater. Chem.*, 2000, 10, 1259–1270.

15 T. W. Sung, Y. L. Lo, *Sensor. Actuat. B.*, 2012, 165, 119–125.

16 M. Darbandi, R. Thomann, T. Nann, *Chem. Mater.*, 2005, 17, 5720–5725.

17 Y. H. Yang, M. G. Gao, *Adv. Mater.*, 2005, 17, 2354–2357.

18 X. X. He, C. Hu, Q. Guo, K. M. Wang, Y. H. Li, J. F. Shangguan, *Biosens and Bioelectron.*, 2013, 42, 460–466.

19 X. Zhao, R. P. Bagwe, W. Tan, *Adv. Mater.*, 2004, 16, 173–176.

20 R. Koole, M. M. van Schooneveld, J. Hilhorst, C. de Mello Donegá, *Chem. Mater.*, 2008, 20, 2503–2512.

21 Z. Zhelev, H. Ohba, R. Bakalova, *J. Am. Chem. Soc.*, 2006, 128, 6324–6325.

22 M. L. Chen, Y. J. He, X. W. Chen, J. H. Wang, *Bioconjugate Chem.*, 2013, 24, 387–397.

23 F. Gao, J. X. Han, C. F. Lv, Q. Wang, J. Zhang, *J. Nanopart. Res.*, 2012, 14, 1191–1201.

24 L. Wang, K. M. Wang, S. Santra, X. J. Zhao, L. R. Hilliard, *Anal Chem.*, 2006, 1, 647–654.

25 K. Khoshmanesh, S. Baratchi, F. J. T. Lopez, *Microfluid Nanofluid.*, 2012, 12, 597–606.

26 C. C. Wang, K. C. Lan, M. K. Chen, M. H. Wang, L. S. Jang, *Biosens and Bioelectron.*, 2013, 49, 297–304.

- 27 L. S. Jang, P. H. Huang, K. C. Lan, Biosens and Bioelectron., 2009, 24, 3637–3644.
- 28 W. H. Yeo, H. B. Lee, J. H. Kim, K. H. Lee, J. H. Chung. Nanotechnology., 2013, 24, 185502-185510.
- 29 L. J. Yang, P. P. Banada, M. R. Chatni, K. S. Lim, A. K. Bhunia, M. Ladisch, R. Bashir, Lab Chip., 2006, 6, 896–905.
- 30 S. T. Selvan, T. T. Tan, J. Y. Ying, Adv. Mater., 2005, 17, 1620-1625.
- 31 S. Q. Wang, C. L. Li, P. Yang, M. Ando, N. Murase. Colloids and Surfaces A: Physicochem. Eng. Aspects., 2012, 395, 24–31.
- 32 Isnaeni, L. H. Jin, Y. H. Cho, J. Colloid. Interf. Sci., 2013, 395, 45–49.
- 33 M. Darbandi, G. Urban, M. Krüger. J. Colloid. Interf. Sci., 2010, 351, 30–34.
- 34 C. Wang, Q. Ma, W. C. Dou, S. Kanwal, G. N. Wang, P. F. Yuan, X. G. Su, Talanta. 2009, 77, 1358–1364.
- 35 M. R. Wang, H. M. Kang, D. Xu, C. Y. Wang, S. Z. Liu, X. Y. Hu, Food Chemistry. 2013, 141, 84–90.
- 36 F. Shahdost-fard, A. Salimi, E. Sharifi, A. Korani, Biosens and Bioelectron., 2013, 48, 100–107.